Experimental Study of the Dynamic Properties of Monolayers of PS−PEO Block Copolymers: The Attractive Monomer Surface Case

Sandrine Rivillon,† Mercedes G. Muñoz, Francisco Monroy, Francisco Ortega, and Ramón G. Rubio*

Departamento de Química Física I, Facultad de Química, Universidad Complutense, 28040 Madrid, Spain

Received August 5, 2002

ABSTRACT: The equilibrium properties of the monolayers of three diblock and two triblock copolymers composed of polystyrene (PS) and poly(ethylene oxide) (PEO), at the air−water interface, have been obtained between 5 and 35 °C. The results have been discussed in terms of the dilute, self-similar layer (SSL) and quasi-brush regimes predicted by scaling and self-consistent-field theories. The SSL to quasi-brush transition was found to be continuous. Below the transition, a master curve was obtained for the isotherms of the diblock copolymers when the area axis was normalized by the number of ethylene oxide groups in the chain. For the two triblock samples, it was not possible to build a master curve. The two copolymers with the largest PS blocks show isotherms that collapse before the brush state was reached. The dynamics of the monolayers was studied using a combination of experimental techniques that has allowed us to obtain data over a broad frequency range: 0.01 Hz to 100 kHz. In all the cases, the dynamic elasticity ϵ was larger than the equilibrium compression modulus, which points out the viscoelastic character of the monolayers. As the SSL structure develops, the number of tails and loops protruding into the subphase increases. These tails and loops are very effective in dissipating the stress, thus leading to a decrease of ϵ until the end of the SSL−quasi-brush transition where, for some block copolymers, the interaction between the stretched PEO chains in the subphase contributes to a further increase of ϵ. Negative apparent dilational viscosities appear for the triblock copolymer with a PS block larger than the PEO ones. The data have been analyzed in terms of two recently proposed dispersion equations. Although one of them is able to reproduce the SQELS spectra without negative apparent dilational viscosities, the molecular meaning of one of the parameters used is not yet clear.

Introduction

Because of their technological and academic interest, monolayers of block copolymers have attracted much attention during the past two decades.[1−10] Two main types of behavior have been distinguished according to the phase transitions that they show:[11] *nonattractive* and *attractive*.

In the nonattractive case the system presents a pancake structure at low surface density Γ. The structure changes to a mushroom-like one at intermediate Γ's. Finally, at higher Γ's the steric interactions between the polymer chains result in an anisotropic stretching of the polymers from the surface, leading to the brush conformation. Both self-consistent-field (SCF) and scaling theories predict scaling laws for the surface pressure Π vs Γ for the mushroom and the brush regimes and also predict the value $\Gamma_b = 4\pi\Gamma R_F^2$ (R_F being Flory's radius) at which the transition takes place ($\Gamma_b = 2$ from SCF).[3,4,11−14] From the experimental point of view, Kent et al. have tested the theoretical predictions with PS−PDMS [polystyrene-*b*-poly(dimethylsiloxane)] at the air−dioctyl phthalate interface.[15−17]

In the *attractive* case a self-similar structure (SSL) or pancake is found at low grafting densities. Increasing Γ, the steric interactions force the chains to protrude into the solution, and a quasi-brush is formed. According to Alexander[1] and Ligoure,[13] the pancake-to-brush transition is first-order, while Aubouy et al.[18] concluded that it is a continuous phase transition. In any case, it is predicted that the width of the Γ-interval, through which the transition takes place, depends on the adsorption energy and on the length of the grafted chain. More recently, Szleifer[12] has indicated that in the case of copolymers the nature of the transition is also strongly dependent on the repulsion energy between the grafted and the grafting chains.[12] The SCF theory predicts Π vs Γ scaling laws for the SSL and the quasi-brush regimes as well as for the segment concentration profile as one moves from the interface to the bulk subphase.[3,11]

Polystyrene-*b*-poly(ethylene oxide) (PS−PEO) copolymers at the water−air interface have been frequently used to test the theoretical predictions.[19−22] Bijsterborsch et al.[19] and Fauré et al.[21,22] have carried out extensive neutron reflectivity experiments on monolayers of PS−PEO. Their copolymers had a molecular weight of PS of ca. 4000, and the molecular weight of the PEO blocks ranged from ca. 4000 to 30 000. The shapes of their isotherms are similar to those reported by Gonçalves da Silva et al.[20,23] The reflectivity data were analyzed in terms of the SCF theory.[11,21,22] In refs 19−22 it was found that the SCF theory correctly predicts the overall shape of the Π vs Γ curves. They also confirmed the validity of the scaling laws predicted by the theory for the SSL regime, and they pointed out the continuous character of the SSL−quasi-brush transition. Furthermore, they concluded that, for $\Gamma < \Gamma_b$, the surface behavior is dominated by the PEO chains, while the PS block mainly influences the value of Π at which the transition takes place. However, at high values of Γ, the length of the PS block becomes more important,

* To whom correspondence should be addressed. E-mail: rgrubio@quim.ucm.es.
† Current address: Complex Fluids Lab., Cranbury Res. Ctr., Rhodia Inc., Cranbury, NJ 08512-7500.

10.1021/ma021260z CCC: $25.00
Published on Web 05/07/2003

Table 1. Characteristics of the Copolymers Used in This Work[a]

copolymer	M_n(PEO)	M_n(PS)	M_n(PEO)	M_w/M_n	N_{PEO}	N_{PS}
DB1	46 900	6 100		1.05	1066	59
DB2	41 900	11 000		1.04	952	106
DB3	36 400	16 400		1.04	827	158
TB1	3 100	2 800	3100	1.04	70	27
TB2	2 700	18 400	2700	1.07	61	177

[a] $M_n(i)$ is the molecular weight of the i-block, N_i is its number of segments, and M_w/M_n is the polydispersity index of the copolymer.

since the PS segments may completely cover the surface, which would no longer be attractive for the PEO chains.

Dewhurst et al.[24] have also reported neutron reflectivity data for Gibbs monolayers of low-molecular-weight PS-*b*-PEO copolymers [M_w(PS) ≈ 1300, M_w(PEO) = 1800−6750]. They suggested that there is a surface phase separation and criticized the SSL−quasi-brush picture given in refs 11 and 19. A similar conclusion was reached by Cox et al.[25] for diblock copolymers in which M_w(PS) > M_w(PEO). Moreover, Malzert et al.[9] have also criticized the SSL−quasi-brush transition in an analysis of neutron reflectivity data of poly(methyl methacrylate)-*b*-polystyrene monolayers.

Although the dynamic surface properties can be especially important from the point of view of applications, only a few studies have been devoted to the dynamics of copolymers adsorbed at the air−water interface.[26−30] Very recently, Noskov et al.[31] have measured the dilational elasticity and viscosity of monolayers, over a broad frequency range, for one of the PS-*b*-PEO copolymers studied by Fauré et al.[21,22] Their results can be explained in terms of the existence of three regimes in the monolayer as Γ is increased: dilute, SSL, and quasi-brush. In the high-frequency regime their results are similar to those of Cao and Kim for PEO[32] and those of Milling et al. for poly(butadiene)-*b*-PEO copolymers.[33] However, the analysis of the capillary-wave data in the quasi-brush regime is more complex, since the in-plane shear viscosity might be comparable to the dilational viscosity due to the high viscosity of the interfacial region.[31]

The purpose of this paper is twofold: on one hand, we will expand the study of the equilibrium behavior of monolayers of three PS-*b*-PEO diblock copolymers with larger PS blocks than those already studied in the literature. We will also expand the study to include two PEO−PS−PEO triblock copolymers. Monolayers of these triblock copolymers have not been studied previously. On the other hand, we will measure the dynamics of the monolayers over a broad frequency range using capillary wave methods. The viscoelastic moduli obtained will be discussed in terms of new dispersion equations, using the information obtained from the equilibrium data.

Experimental Section

Materials. Diblock (poly(styrene−ethylene oxide) (PS−PEO)) and triblock (PEO−PS−PEO) copolymers used in this investigation were prepared by anionic polymerization and purchased from Polymer Source (Dorval, Canada). Table 1 summarizes the characteristics of the copolymers used. All the samples were insoluble in water.

The solvent used for preparing the diblock and triblock copolymer solutions was a mixture of chloroform and benzene (1:1). This mixture is selective for both polymers, it is quite volatile, and it has good spreading characteristics on a water surface. The polymer concentration of the spreading solutions was 10^{-3} M in monomers. Most of the experiments were performed between 5 and 35 °C.

Double distilled and desionized water from a Milli-Q-RG unit has been used in all the experiments. Its resistivity was always higher than 18 mΩ cm^{-1}. Before spreading the polymer solutions, the surface tension of water was checked by the plate method to be sure that there were no surface-active impurities. Also, the chloroform + benzene mixture was spread in order to ensure that it did not contain any surface active impurities.

Langmuir Balance. The spread monolayers were formed on a commercial Teflon Langmuir trough (KSV Instruments minitrough model, Finland). A Pt Wilhelmy balance placed at the air−water interface was used as the surface force sensor. Two polyoxymethylene barriers were placed from each side of the trough to allow the oscillating barriers study (see below). The temperature of the monolayers was controlled by passing thermostated water through the jacket of the trough. Near the interface, the temperature was measured with a precision of 0.01 °C, and the temperature control was better than ±0.05 °C.

For each experiment, the surface concentration Γ was increased by subsequent additions of the polymer solutions using a Hamilton microsyringe. After solvent evaporation, equilibration times of at least 10 min were required before the surface pressure was measured (more than 1 h was necessary for Γ > Γ$_b$). Each Π value was determined with a 0.1 mN m^{-1} precision.

Ellipsometry. A Plasmos SD2300 ellipsometer (Germany) with an automated rotating analyzer system was used for this study. The incident monochromatic He−Ne laser beam (λ = 632.8 nm) was concentrated on a 30 × 30 μm surface. To improve the sensitivity of the measurement, the incident angle (θ = 55°) was chosen close to the Brewster angle (52° for water). Two ellipsometric angles Ψ (related to the change in intensity between the incident and the reflected beams) and Δ (the phase shift) were obtained from these measurements. The ellipsometry experiments were performed only at 22 °C.

Surface Hydrodynamics. The hydrodynamic motions in the polymer monolayers can be divided in two main modes: the capillary—out of plane—and the longitudinal—in plane—modes. The capillary mode is essentially a shear motion that is driven by the surface tension [$\tilde{\gamma}(\omega) = \gamma + i\omega\mu$, where γ is the surface tension and μ the transverse viscosity]. However, the longitudinal mode contains both in-plane shear and compression contributions, each one characterized by an elastic modulus. Thus, the viscoelasticity is the sum of both contributions: $\tilde{\epsilon}(\omega) = \epsilon_s + \epsilon_K = \epsilon + i\omega\kappa$, where ϵ is the dilational elasticity and κ is the dilational viscosity of the system.

To study the dynamical properties of the copolymers monolayers in a large frequency range ($10^{-2} < \omega < 10^6$ Hz), we have used different techniques: oscillating barrier experiments, electrocapillary waves (ECW), and surface quasi-elastic light scattering (SQELS). These techniques were the same as ones described in previous papers.[34,35] At low frequency ($\omega < 10^1$ Hz), oscillating barrier experiments have been performed on a Langmuir trough by moving a barrier under computer control. In these kinds of experiments, the frequency of the oscillations is varied for a given area. From the experimental parameters, both the real and the imaginary components of the dilational elastic modulus can be calculated.[34]

At higher frequencies (ω > 100 Hz), two other methods have been used: ECW and SQELS. In the first case, the surface capillary waves at the air/water interface were excited by the application of an electric ac field (∼500 V) through a blade positioned within 100 μm of the interface. The wave vector q and the corresponding spatial damping coefficient β were determined by optical reflectometry of a laser beam positioned at various distances from the blade. These two parameters were then used to obtain the dilational elasticity and viscosity. In the SQELS technique, a polarized He−Ne laser beam passed through a spatial filter that expanded the beam and ensured a Gaussian intensity profile. The beam then passed through a transmission diffraction grating (Align-Rite, UK), and a 1:1 image of the grating was formed on the monolayer. The light scattered by the capillary waves was detected in the

heterodyne mode. The wave vector was selected by focusing each one of the diffraction spots into the photomultiplier. The signal was collected and analyzed by a Stanford research (USA) model 760 FFT spectrum analyzer.

In both cases, dilational elasticity ϵ and loss modulus $\omega\kappa$ were estimated from the dispersion equation[36]

$$D(\omega) = L(\gamma)\, T(\tilde{\epsilon}) - C(\rho,\eta) \equiv 0 \tag{1}$$

where

$$L(\tilde{\epsilon}) = \tilde{\epsilon} q^2 + i\omega\eta(q + m) \tag{2}$$

$$T(\gamma) = \gamma q^2 + i\omega\eta(q + m) - \frac{\rho}{q}\omega^2 + \rho g \tag{3}$$

ρ and η are the liquid density and viscosity, respectively, and m^{-1} is the capillary penetration depth:

$$m^2 = q^2 + \mathrm{i}\omega\frac{\rho}{\eta}, \quad \text{with } \mathrm{Re}(m) > 0 \tag{4}$$

$C(\rho,\eta) = [i\omega\eta(q - m)]^2$ is the coupling term which accounts for the bulk hydrodynamic coupling between the capillary and the dilational modes, mediated by the 3D phases.

The spectrum of the scattered light by thermally excited capillary waves is given by

$$P_z(q,\omega) = -\frac{2k_B T}{\pi\omega}\,\mathrm{Im}\left[\frac{\tilde{\epsilon} q^2 + i\omega\eta(q + m)}{D(q,\omega)}\right] = -\frac{2k_B T}{\pi\omega}\,\mathrm{Im}\left[\frac{L(\tilde{\epsilon})}{D(q,\omega)}\right] \tag{5}$$

It is known that experimental spectra appear broadened because of instrumental contributions and that the experimental spectra correspond to a convolution between the theoretical spectrum and an instrumental function, $G(\omega)$. In our experimental technique, $G(\omega)$ can be accurately described by a Gaussian function.[34] Consequently, the experimental spectra must be fitted to

$$P(q,\omega) = \int P_z(q,\omega')\, G(\omega - \omega')\, \mathrm{d}\omega' \tag{6}$$

In all of the above formulas, $\tilde{\epsilon} = \epsilon + i\omega\kappa$ and $\tilde{\gamma} = \gamma + i\omega\mu$, where ϵ is the dilational elasticity, κ is the dilational viscosity, γ is the surface tension, and μ is the transverse viscosity, which has been shown to be zero for fluids. We have found that the values of γ obtained from the SQELS spectra are equal to the equilibrium values within their combined uncertainty.

Results and Discussion

Equilibrium Results. Figure 1 shows the surface pressure Π vs area A for the three copolymers at 295 K. The area per chain axis has been normalized by N_{PEO}, the number of ethylene oxide units in the PEO block. Also, the results obtained for a sample of PEO homopolymer (M_w = 35 000) are shown for the sake of comparison. The Π vs A curves of the diblock copolymers are similar to those reported in refs 19−23. It can be observed that the three curves overlap until reaching the pseudo-plateau when they are scaled with N_{PEO}. This is in agreement with previous conclusions of Currie et al.[11] and of Fauré et al.[21,22] This behavior is expected for the SSL regime of grafted chains attracted to the interface. The dilute regime, which can be described by a scaling law $\Pi \sim \Gamma^2 \sim A^{-2}$, is not observed in our experiments. This can be explained by a discussion of the area at which the PEO chains start to contact each other. For good solvent conditions, this area can be calculated as $A^* = \pi R f^2/4$, with the Flory's radius of gyration given by $R_f \approx aN^{3/4}$ (a = 2.4 Å for PEO).[3] This

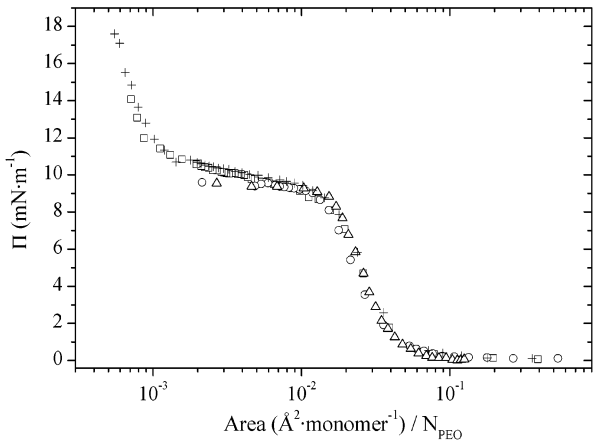

Figure 1. Surface pressure Π vs area per molecule for the three diblock copolymers and a sample of PEO homopolymer (M_w = 35 000). The area axis has been normalized with the number of EO segments N_{PEO} in each molecule. The data shown correspond to 25 °C. Symbols: □, DB1; +, DB2; ○, DB3; △, PEO. Similar results were obtained at other temperatures.

leads to $A^*/N_{PEO} > 0.1$ Å^2 for the three diblocks studied in this work, a value that is close to the point where the Π values start to increase in Figure 1, and thus is in good agreement with the value of $A^* = 1/\Gamma^*$ calculated from the ln Π vs ln A curves. Moreover, this leads to values of $1.8 < \Gamma_b/\Gamma^* < 2.5$, which are relatively close to the value predicted by the SCF and scaling theories $\Gamma_b/\Gamma^* = 2$.

At higher grafting densities (semidilute regime), it is predicted that $\Pi \sim \Gamma^y$, with y = 2.85 for a 2D system (y = 2.25 for a 3D system) under good-solvent conditions and y = 2.25 for poor-solvent conditions. The best fit of the ln Π vs ln A results leads to $y = 2.36 \pm 0.01$ for DB1, 2.32 ± 0.02 for DB2, 2.14 ± 0.05 for DB3, and 2.54 ± 0.08 for the PEO homopolymer. These results are similar to those of Fauré et al.,[22] who found $2.85 > y > 2.25$ for their diblock copolymers. This indicates that the chain conformation is intermediate between purely 2D entangled layer and a 3D interpenetrated layer.

The values of the area at which the system crosses over from the semidilute to the concentrated regime are larger than 100 000 Å^2/chain for the three diblocks, while the area occupied by the PS chains is lower than 300 Å^2/chain. Therefore, at the crossover point the PS blocks do not form a continuous layer. Moreover, from the projected areas of the PEO and the PS blocks and the area at the crossover point, one can conclude that, at this point, at least 36% of the PEO monomers are adsorbed at the interface. This percentage is lower than the one reported by Fauré et al.[23] from neutron reflectivity experiments for PEO−PS diblocks of lower molecular weight (up to 80%). However, one cannot forget that the scaling laws used for the present calculations lack numerical factors that can affect the final results.

The effect of increasing N_{PS} is very small in the semidilute regime and, within the experimental uncertainty, does not change the height of the pseudo-plateau (Π_{Pl}) for DB1, DB2, and DB3. However, even the moderate increase of N_{PS} from DB2 to DB3 leads to nonnegligible decrease of the slope of the plateau. Fauré et al.[23] have argued that the effect of the length of the PS block upon the slope of the pseudo-plateau indicates that the PS blocks behave as a fluid in a poor solvent (the air−water interface). Again, using the projected areas of the PS and PEO chains, it can be calculated

that, for the DB1 and DB2 samples, at least 8% of the PEO monomers are adsorbed at the interface at the low-area end of the plateau. Therefore, the beginning of the increase in surface pressure in the high grafting-density region would be due to the repulsion of the PEO chains in the brush. As a consequence, no differences should be expected between the DB1 and DB2 copolymers in the quasi-brush region due to their similar values for N_{PEO}. In fact, the surface pressure in this regime can be considered to be the sum of two contributions: a constant pressure Π_{Pl} resulting from the monolayer of adsorbed segments of constant density and an increasing surface pressure $\Pi_b = \Pi - \Pi_{Pl}$ due to the formation of the brush. Currie et al.[11] used $\Pi_{Pl} = 9.8$ mN m^{-1}, while from Figure 1 we have found $\Pi_{Pl} = 9.0 \pm 0.2$ mN m^{-1}. SCF theory predicts $\Pi_b \sim \Gamma^x$ for long grafted chains, with x being an exponent different from the one that characterizes the crossover from the diluted to the semidilute regimes. This behavior was corroborated by Currie et al.[11] for $N_{PEO} = 700$ ($N_{PS} = 38$) and by the present data for DB1 and DB2.

In the highest grafting-density region, where Π rises sharply, Fauré et al.[23] have shown that, for a copolymer with $N_{PS} = 31$ and $N_{PEO} = 700$, the surface is covered by a continuous layer of fluid PS on top of a quasi-brush formed by the PEO chains. In this situation the interface would no longer be attractive for the PEO chains, and a depletion layer would develop. The DB1 and DB2 samples have larger PEO and PS blocks than those used in ref 23; thus, it is reasonable to assume that a similar picture is valid for these two copolymers for pressures above Π_{Pl}. However, from the equilibrium results, it is not possible to conclude whether the PS layer is in the fluid or in the glassy state.

The collapse of the DB3 monolayer at $\Pi \approx \Pi_{Pl}$ has not been reported in previous studies of PS−PEO diblock copolymers, probably because of the shorter length of the PS blocks used by other authors. In the high grafting region, the shape of the isotherm of DB3 is similar to the one reported for poly(4-hydroxystyrene) ($M_w = 11\,000$), which was found to be glassy at 25 °C.[35] The lack of an increase of Π above Π_{Pl} seems to indicate that the behavior of the monolayer is dominated by the PS layer.

Dorgan et al.[37] have found important differences between the adsorption behavior of triblock and diblock copolymers and have concluded that, in terms of scaling laws, triblock copolymers behave as strongly asymmetric diblock copolymers. Figure 2 shows the results obtained for the monolayers of the two triblock copolymers studied in this work. The curve corresponding to the diblock DB3 has also been included for the sake of comparison. It can be observed that, when normalized by N_{PEO}, the curves for the triblock copolymers are more expanded that those of the diblocks previously discussed, and the two curves do not overlap in the semidilute region. This seems to indicate that, contrary to the monolayers of the diblock copolymers, the PEO chains do not determine the behavior of the monolayer, but the PS segments also play an important role. As in the case of the diblock copolymers, the increase of N_{PS} does not change Π_{Pl}, which takes the same value as in the diblocks. The slope of the pseudo-plateau is larger for the TB1 sample than for the TB2 and for the diblocks. This might in part be due to the fact that N_{PEO} is much smaller for the TB1 and TB2 samples than for the diblocks and that in TB2 the size of the PEO block

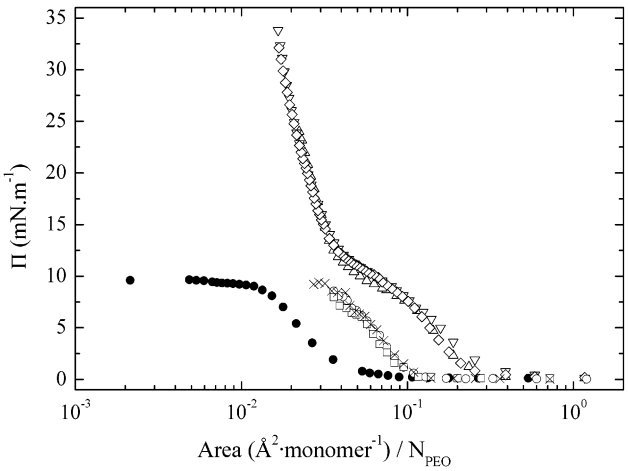

Figure 2. Surface pressure Π vs area per molecule for the two triblock copolymers and a the DB3 diblock copolymer. The area axis has been normalized with the number of EO segments N_{PEO} in each molecule. Symbols: ●, DB3 at 25 °C; △, TB1 at 5 °C; ◇, TB1 at 25 °C; ▽, TB1 at 35 °C; ×, TB2 at 10 °C; ○, TB2 and 25 °C; □, TB2 at 35 °C.

is smaller than that of the PS one. It must be mentioned that the TB2 monolayers become unstable for area/$N_{PEO} \approx 0.03$ Å^2, i.e., at the beginning of the pseudo-plateau. The critical exponent y is quite different for the two triblock copolymers: 2.8 ± 0.3 for TB1 and 4.5 ± 0.4 for TB2. These results indicate that the air−water interface is not a good solvent for the TB2 copolymer, suggesting that in this case (as with DB3) it is the PS block which dominates the behavior of the monolayer.

Figure 2 also shows that temperature has a very small effect in the surface behavior of these triblock copolymers. Similar results were found for the two diblock samples (not shown). In principle, this might appear somewhat surprising because the scaling laws predicted by the SCF theory are, in fact, in the form $\Pi/T \sim \Gamma^y$. However, it can be easily determined that for narrow temperature ranges (where one can assume that y is constant) $d\Pi/dT \sim \Pi/T$, and thus Π/T is lower than 0.03 mN m^{-1} K^{-1} for $\Pi \leq \Pi_{Pl}$. For PEO homopolymer, Kuzmenka and Granick[38] found that in the semidilute regime the temperature coefficient of Π is positive and reaches a constant value at the pseudo-plateau.

Gonçalves da Silva et al.[20,23] found important hysteresis effects in some PS-*b*-PEO copolymers. Fauré et al.[22] also reported hysteresis in the brush regime. As an example of this, Figure 3 shows that the hysteresis cycle found for the TB1 sample is rather small. Similar effects were found for the DB1 copolymer, while the Π vs A curves did not show hysteresis for the DB2 and TB2 copolymers. Our results are similar to those of Fauré et al.[22]

Figure 4a shows the compressibility modulus $\epsilon_0 = d\Pi/d \ln \Gamma$, calculated from the surface pressure isotherms for the three diblock copolymers. The data show a slight temperature dependence for $\Pi < 10$ mN m^{-1}, with ϵ_0 increasing from 10 to 25 °C in both diblock and triblock copolymers. For higher surface pressures, ϵ_0 remains temperature independent within the experimental uncertainty (ca. ± 0.5 mN m^{-1}). The existence of a maximum separated by two surface concentrations for which $\epsilon_0 \approx 0$, and a further increase of ϵ_0 for copolymer presenting a brush region, has been discussed in detail by Noskov et al. for PS−PEO diblock copolymers.[31] The increase of ϵ as Π is increased in the

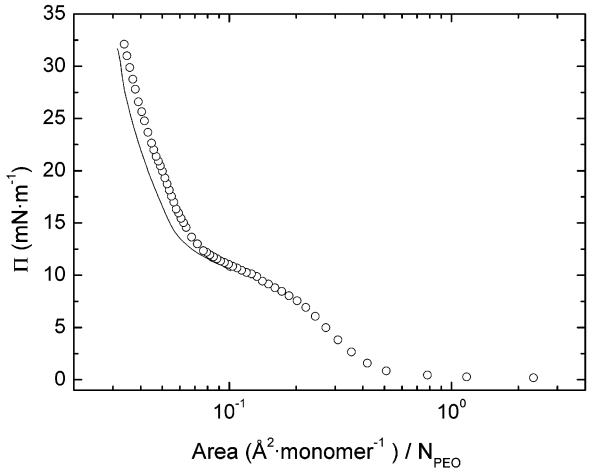

Figure 3. Hysteresis cycle for the monolayer of the TB1 triblock copolymer at 25 °C. The symbols represent the isotherm obtained by subsequent addition of copolymer amounts to the air−liquid interface and waiting for the evaporation of the solvent and the equilibration of the monolayer. The line represents the continuous expansion of the monolayer. Notice that, except for the brush regime, the hysteresis is negligible. Similar results were found for the DB1 and DB2 samples.

semidilute regime is due to the enhancement of the interactions of the PEO chains in the SSL configuration. After reaching its maximum, the decrease of ϵ is due to the increase of loops, trains, and tails of PEO protruding into the subphase, until the point at which the SSL−quasi-brush transition takes place and $\epsilon \approx 0$. In the case of the DB1 and DB2 copolymers, a further increase of area is accompanied by the stretching of the PEO chains in the quasi-brush structure.

The results for the TB1 and TB2 samples (Figure 4b) were similar to those of the diblocks. No explanation can be given for the local minimum found at $\Pi \approx 21$ mN m^{-1} for the TB1 sample. It is worthwhile noticing the similarity of ϵ_0 for the present copolymers and that of the PEO sample for the $\Pi < 10$ mN m^{-1} range, which supports the idea that in the dilute regime, and in the SSL structure, the equilibrium thermomechanical behavior of the monolayers is dominated by the PEO chains. This has also been found by Noskov et al.[31] for a PS−PEO diblock and by Milling et al.[33] for a polybutadiene−PEO diblock.

Ellipsometry allows one to estimate the thickness, *d*, of the monolayer.[39] To calculate the thickness, *d*, of the interface from the ellipsometric angles, we have used the two-layer model described in ref 40: A swollen brush, made only of hydrophilic PEO blocks is immersed in the subphase, and a thin film of PS and PEO lies adsorbed at the air−water interface. The composition of the top layer is calculated assuming that all the PS remains in that layer, while the amount of PEO is calculated from the total area and the projected areas of the PS and PEO blocks. The precision of the calculated thickness is ca. ±2 Å. Figure 5 shows the values of *d* for the DB1 and DB3 copolymers. It can be observed that the film thickness of the DB1 and DB3 copolymers is similar for $\Pi < \Pi_{Pl}$. As the monolayer is compressed through the pseudo-plateau, the diblock with larger N_{PS} forms a much thicker layer up to the collapse of the monolayer at $\Pi \approx \Pi_{Pl}$. However, for the diblock with smaller N_{PS}, the thickness increases very slightly along the pseudo-plateau and then probably grows faster as the brush is compressed. (This region could not be reached in our experiments.) The results for DB2 and TB1 are similar to those of DB1, while those of TB2 are like those of DB3.

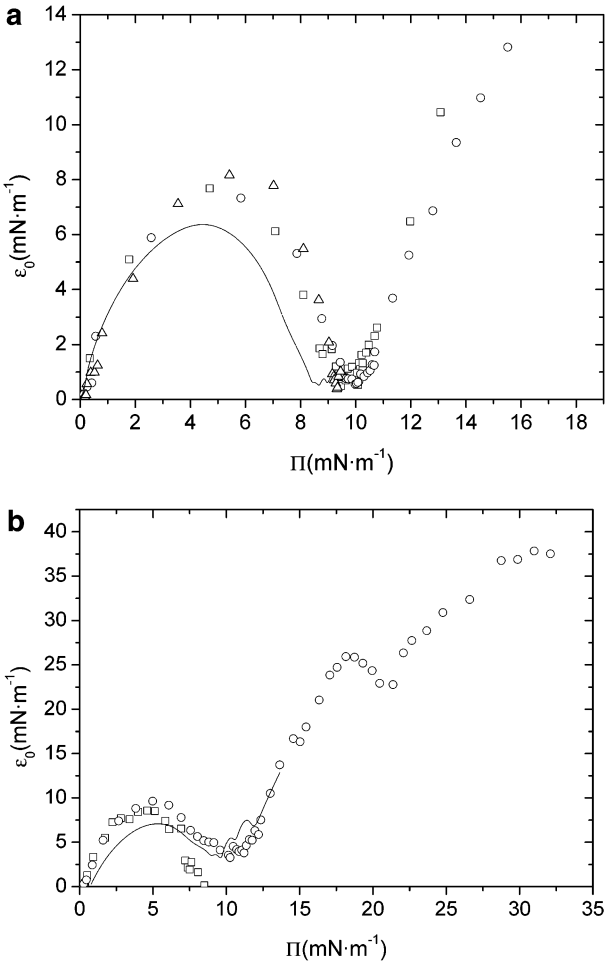

Figure 4. (a) Equilibrium compressibility coefficient ϵ_0 as a function of the surface pressure Π for the PS-*b*-PEO monolayers at 25 °C. Symbols: □, DB1; ○, DB2; △, DB3. The continuous line represents gives the compressibility of the DB1 copolymer at 10 °C. (b) Equilibrium compressibility coefficient ϵ_0 as a function of the surface pressure Π for the PEO-*b*-PS-*b*-PEO monolayers at 25 °C. Symbols: ○, TB1; □, TB2. The continuous line represents gives the compressibility of the TB1 copolymer at 10 °C.

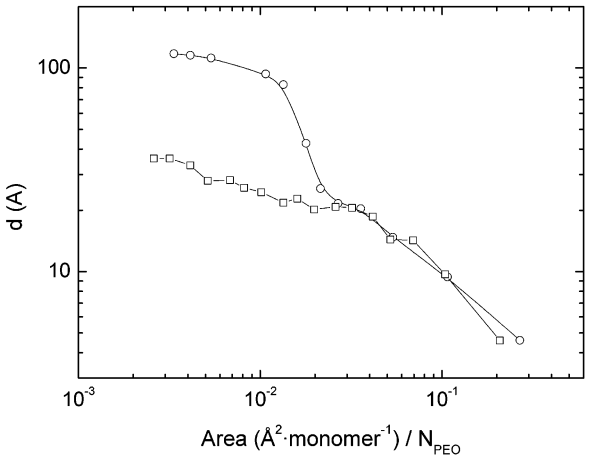

Figure 5. Ellipsometric thickness of the monolayers of DB1 (□) and DB3 (○) at 22 °C. The arrows indicate the SSL−quasi-brush transition region. The results of DB2 and TB1 are very similar to those of DB1, while those of TB2 are similar to those of DB3.

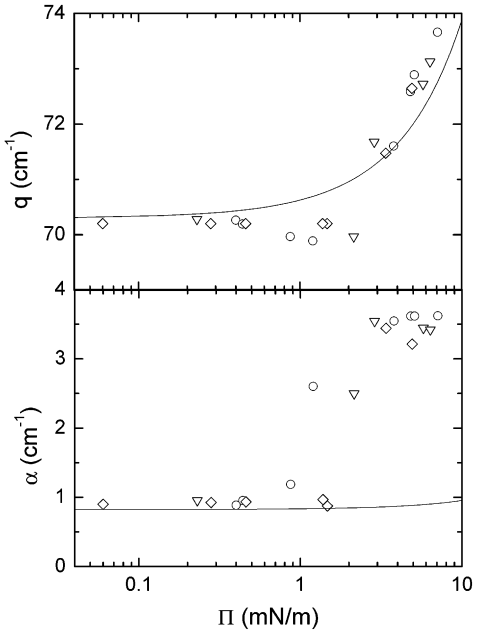

Figure 6. Surface pressure dependence of the wavevector (q) and spatial damping (α) obtained from the ECW experiments for the monolayers of (○) DB1, (◇) DB2, and (▽) DB3 at 25 °C and at a frequency $\omega = 5$ kH. The continuous lines represent the behavior expected from the Kelvin and Reynolds laws, respectively, using the equilibrium surface tension and the density and viscosity of the subphase.

Dilational Rheology. Figure 6 shows the wavevector q and the spatial damping α for the electrocapillary waves of three monolayers excited at $\omega = 5$ kHz. As can be observed, near $\Pi = 1$ mN m^{-1} there is an important increase in both magnitudes. $\Pi = 1$ mN m^{-1} roughly corresponds approximately to the grafting density at which the system crosses over from the dilute to the semidilute regimes. Similar plots were obtained for the crossover from the semidilute to the concentrated regimes and for the other diblock and triblock copolymers. These results are similar to those reported by Noskov et al.[31] for a PS−PEO diblock copolymer, although they explored a higher grafting density range. The continuous lines represent the values calculated from the limit laws of Kelvin and Reynolds using the equilibrium surface tension and the density and viscosity of the subphase. We can be observed that, while the wavevector is predicted reasonably well, the damping is strongly underestimated. Reynolds' law considers that the viscosity of the subphase is the parameter that controls the energy dissipation of the interface. The α results show that in order to account for the spatial damping one needs an effective viscosity much larger than that of the subphase. Therefore, other energy dissipation mechanisms, not accounted for by Kelvin's and Reynolds' laws, must exist in the monolayers. The viscoelastic character of polymer monolayers has already been pointed out in the literature.[31,33−35]

Figure 7 shows representative examples of the SQELS spectra obtained for two monolayers. Similar results were obtained for other monolayers at different surface concentrations. We have fitted the spectra to eq 6.[36] When the analysis of the frequency of the maximum and of the half-width at half-height are discussed in terms of Kelvin's and Reynolds' laws, the conclusions are the same than those mentioned above for the results of the electrocapillary waves experiments.

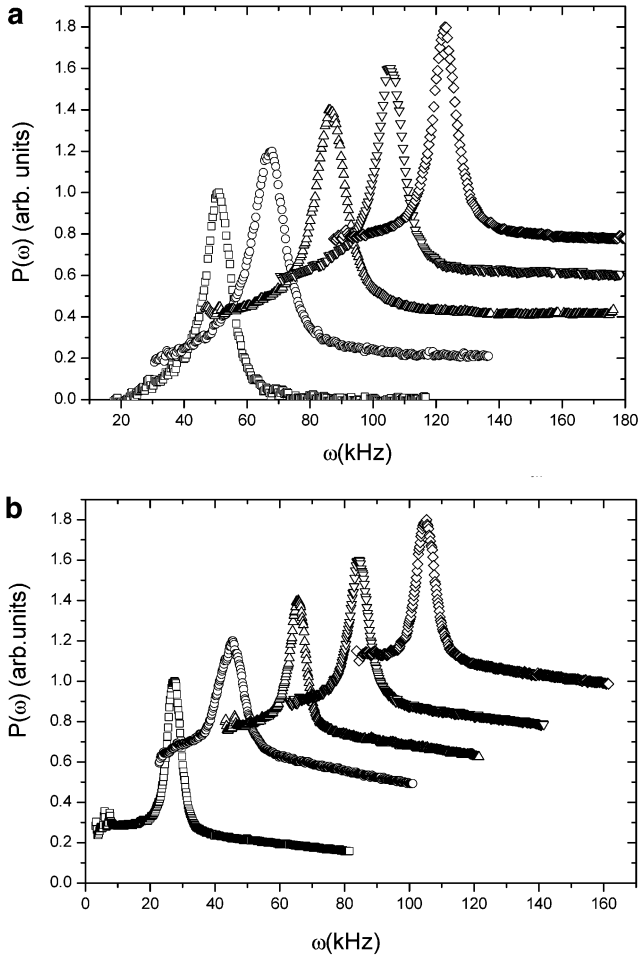

Figure 7. (a) Surface pressure dependence of the spectra of scattered light by thermal capillary waves SQELS for the monolayer of DB1 at 25 °C. The wavevector is $q = 334.5$ cm^{-1}. For the sake of clarity, the spectra have been shifted 20 kHz in the frequency axis and 0.2 au in the ordinate axis. Symbols correspond to different values of Π in mN m^{-1}: □, 2.1; ○, 4.1; △, 7.0; ▽; 8.4; ◇; 10.6. (b) Surface pressure dependence of the spectra of scattered light by thermal capillary waves SQELS for the monolayer of TB1 at 25 °C. The wavevector is $q = 223.4$ cm^{-1}. For the sake of clarity, the spectra have been shifted 20 kHz in the frequency axis and 0.2 au in the ordinate axis. Symbols correspond to different values of Π in mN m^{-1}: □, 1.2; ○, 4.7; △, 8.5; ▽; 12.7; ◇; 14.8.

Figure 8 shows the surface pressure dependence of the dynamic elasticity ϵ calculated from the ECW experiments at $\omega = 5$ kHz for the diblock monolayers. Similar results were obtained at other frequencies (including those of the SQELS experiments) and for the triblock copolymers.

The first point to notice is that $\epsilon > \epsilon_0$ even at low values of Π. These results are similar to those found by Noskov et al.[31] for a diblock PS−PEO copolymer and for other polymer monolayers.[34,35,40] In all these cases, the difference $(\epsilon - \epsilon_0)$ is accompanied by the existence of nonnegligible values of the dilational viscosity, thus pointing out the viscoelastic character of the monolayers. As discussed previously, the behavior of the monolayers of the DB1 and DB2 copolymers is mainly dominated by the PEO segments up to surface pressures beyond the SSL−quasi-brush transition. However, for the DB3 sample, a continuous layer of PS seems to be formed in the plateau of the Π vs area curve. Although no differences between the behavior of the three samples are observed in Figure 8, they will become apparent

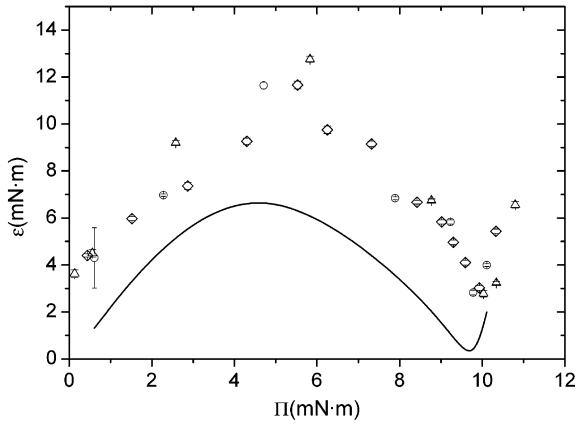

Figure 8. Pressure dependence of the elasticity modulus at $\omega = 5$ kHz (ECW) and 25 °C for monolayers of the diblock copolymers. Symbols: ○, DB1; △, DB2; ◇, DB3. The continuous curve represents the equilibrium elasticity of DB1.

when the frequency dependence of the viscoelastic moduli was discussed.

We have tried to calculate the value of y in the $\Pi \sim y\epsilon(\omega)$ dynamic scaling law in the semidilute regime, and although the scattering of the results leads to a large uncertainty, the comparison with the values obtained from the equilibrium data ϵ_0 data indicates that the agreement is acceptable for DB1, DB2, and TB1. For DB3 and TB2 the value of y obtained from ϵ is larger than that obtained from ϵ_0 (e.g., for TB2 $y = 8 \pm 1$ from ϵ, while 4.5 ± 0.4 from ϵ_0). These results contrast with previous results for insoluble monolayers of slightly polar homopolymers, where the same values of y were obtained from the static and the dynamic compressibility data.[41]

A comparison of the results shown in Figure 1 with those of Figure 8 points out that, in the semidilute regime, $\epsilon/\gamma < 0.2$. This means that the capillary wave experiments carried out in this work are not far from the resonance conditions of the capillary and the dilational modes.[36] Therefore, in analyzing the frequency dependence of our results, one can safely consider that the frequencies of both modes are close to each other in this grafting regime. Such an assumption would not be valid for the DB1, DB2, and TB1 copolymers at the highest grafting densities studied (see Figure 4).

Figure 9 shows the frequency dependence of the dynamic compressibility $\epsilon(\omega)$ and of the loss modulus $\omega\kappa(\omega)$ for the DB1 and TB1 monolayers at the grafting density Γ**, i.e., the crossover from the semidilute to the concentrated regimes [Π(Γ**)/mN m^{-1} = 4.7, DB1; 6.0, DB2; 7.2, DB3; 4.9, TB1; 2.1, TB2]. In this figure we have also included the results obtained from oscillatory barrier experiments in the frequency range 0.01−0.2 Hz. The results show that there is a viscoelastic relaxation in the 0.01 Hz−100 kHz range, whose shape can be roughly described by a Maxwell relaxation with a characteristic time of the order of 10 ms. The fact that $\epsilon \approx 0$ (with a ±2 mN m^{-1} uncertainty) in the low-frequency range can be easily understood since Γ** is close to the SSL−quasi-brush transition (see Figure 4), where the value of ϵ_0 is small. The values of loss modulus $\omega\kappa$ obtained in the semidilute regime are small for the DB1, DB2, and TB1 samples. In the 10^2-10^4 Hz frequency range, the maximum of $\omega\kappa$ tends to increase with the grafting density, although the experimental uncertainty is high. As can be observed in Figure 9, the loss modulus can be roughly described by a Maxwell

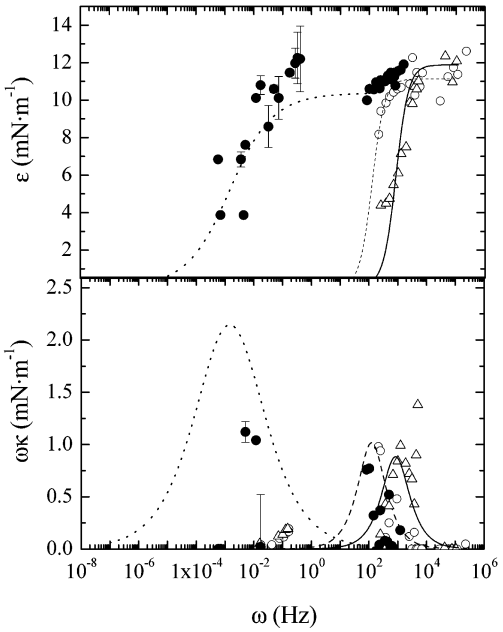

Figure 9. Frequency dependence of the dynamic elasticity modulus ϵ and the loss modulus $\omega\kappa$ for monolayers of DB1 (○), TB1 (△), and a $PEO_{76}-PPO_{29}-PEO_{76}$ copolymer (●) (PPO = poly(propylene oxide)) at 25 °C and at a grafting density Γ** corresponding to the crossover from the semidilute to the concentrated regimes. The lines represent the fit of the data to a Maxwell relaxation for the DB1 and TB1 monolayers and to a Lucassen−van den Temple process for the PEO−PPO−PEO monolayer. In the case of DB1 and TB1, the amplitude of the Maxwell relaxation that fits the elasticity is larger than that needed for fitting the loss modulus.

mode, with the same relaxation time used to describe the $\epsilon(\omega)$ curves. However, it is important to note that different amplitudes of the Maxwell mode are necessary in order to describe the real and the imaginary components of the viscoelastic modulus. This may be due in part to the fact that the resonance condition between the capillary and the dilational modes is not exactly fulfilled or to the fact that the Maxwell mode is too simple to describe the dynamic processes at the interface.

Noskov et al.[31] have discussed their results of ECW and longitudinal waves in the semidilute regime of a PS−PEO diblock copolymer in terms of the reptation theory of Noskov.[43] They claimed that the dynamics of exchange of EO monomers between the surface and the subsurface is fast compared to the in-plane reorganization of the SSL structure. As a consequence, they suggested that such dynamics should appear at frequencies above 10 kHz for their diblock copolymer. Moreover, in a recent work on Gibbs monolayers of PEO,[44] the same authors concluded that the adsorption−desorption dynamics lies in the 10 Hz−1 kHz range. On the basis of this finding, and considering the similarity of the equilibrium behavior of the PS−PEO copolymers and the PEO homopolymer in the semidilute regime (see Figure 1), one might be tempted to assign the relaxation mode observed in Figure 9 to this adsorption−desorption process.

Milling et al.[33] and Noskov et al.[31] have suggested the existence of low-frequency ($\omega < 1$ Hz) relaxation processes in monolayers of PEO containing diblock copolymers. A low-frequency relaxation process was also suggested for PEO−poly(propylene oxide)−PEO ($PEO_{xx}-PPO_{yy}-PEO_{xx}$) copolymer.[42] Within the precision of the

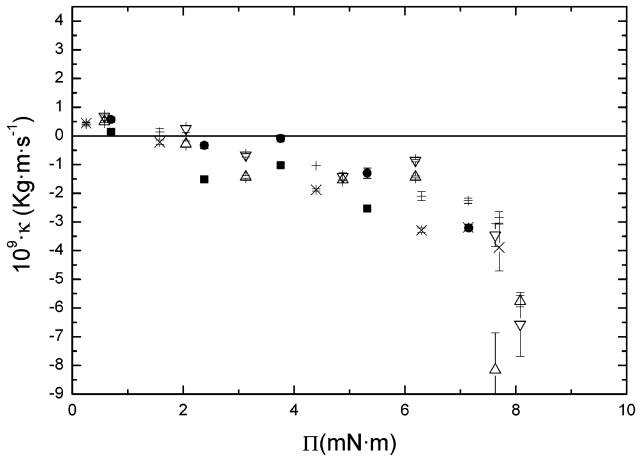

Figure 10. Dilational viscosity of the monolayers of TB2 as a function of the surface pressure. Symbols: ■, 10 °C and q = 334 cm^{-1}; ●, 10 °C and q = 223.4 cm^{-1}; △, 25 °C and q = 334 cm^{-1}; ▽, 25 °C and q = 223.4 cm^{-1}; ×, 35 °C and q = 334.5 cm^{-1}; +, 35 °C and q = 223.4 cm^{-1}.

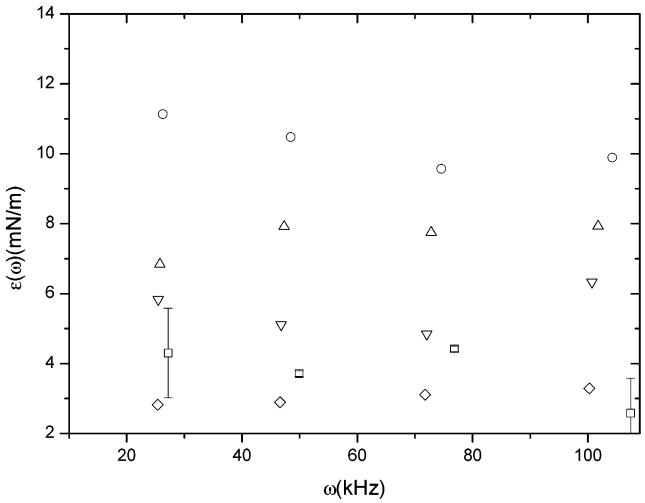

Figure 11. Frequency dependence of the dynamic elasticity, in the high-frequency region and for different values of the surface pressure Π (mN m^{-1}): □, 0.61; ○, 4.77; △, 7.89; ▽, 9.23; ◇, 9.78. The bars represent the uncertainty of ϵ at the different frequencies.

data for our samples, no such low-frequency dynamics is observed in the SSL structure for the DB1, DB2, DB3, and TB1 monolayers.

The relaxation process observed can be assigned to the adsorption−desorption of short segments of the PEO blocks, a process that can be accompanied by the in-plane reorganization of the monolayer. (Even at the plateau region, there is a noticeable amount of PEO segments adsorbed at the surface.) The adsorption−desorption of large PEO segments cannot appear in the 10^0−10^4 Hz range. To illustrate this point, Figure 9 shows the long- and short-PEO segment dynamics for a related copolymer: PEO_{76}−PPO_{29}−PEO_{76}. While the short-segment dynamics appears between 10^0 and 10^2 Hz, the long-segment dynamics is centered in the millihertz range. This later process can be well described by the Lucassen−van den Tempel model,[45] with a relaxation time of $\tau \approx 1000$ s, very close to the corresponding value obtained from the analysis of adsorption dynamics of solutions of PEO−PPO−PEO.[42] Although the low-frequency dynamics, related to adsorption, does not appear in the five samples studied in this work, it might appear in low-molecular-weight soluble PS−PEO copolymers.

The most striking result is that for the DB3 and the TB2 samples the loss modulus has negative apparent values. Figure 10 shows some representative results for TB2. It can be observed that the dilational viscosity takes negative apparent values as the grafting density is increased slightly beyond the value Γ** [Π(Γ**) = 0.04 mN m^{-1} for TB2], i.e., the crossover from the dilute to the semidilute regimes. The change from positive to negative values of $\omega\kappa$ seems to be independent of the temperature and of the frequency for the DB3 and TB2 copolymers. A similar behavior has been found for Gibbs and Langmuir monolayers of PEO−PPO−PEO,[42] although in this case the change was found for Γ ≈ Γ**, i.e., for surface pressures close to Π_P. Similar negative apparent values of $\omega\kappa$ have been reported for other copolymers.[29]

We have explored the influence of the grafting density on the dynamic elasticity in the high-frequency range. Figure 11 shows representative results for the DB1 monolayer. The results indicate that at high frequencies the monolayer has already relaxed, thus leading to a constant ϵ and to $\kappa = 0$. The Π dependence of ϵ follows the trend already shown in Figure 4. The results obtained at low frequencies (0.01−1 Hz) by the oscillatory barrier method lead to $\epsilon \approx \kappa \approx 0$ for the same values of Π shown in Figure 11.

Comparison with Buzza's Theory.[46] The existence of negative apparent dilational viscosities is one of the key problems in the study of interfacial rheology. Although no clear theoretical answer has been given to this problem, it seems clear that these apparent values arise from the fact that the hydrodynamic description, which leads to the classical dispersion equation used (eq 1), is incomplete. As shown in Figure 5, the thickness of some of the monolayers is quite large. Buzza et al.[46] have pointed out that, in the case of thick monolayers, the capillary and dilational modes are not the only contributions to be taken into consideration. In effect, the bending and splaying modes might make important contributions to the interfacial hydrodynamics of the monolayers due to their coupling to the dilational mode. However, it has been pointed out that only for rather thick monolayers the coupling term between bending and dilational modes can make any significant contribution to the SQELS spectra.[46,47] In view of Figure 5 we have considered that it would be worthwhile to check the ability of Buzza's dispersion equation to describe the data of the DB3 and TB2 monolayers. When the bending mode is taken into account, Buzza's dispersion equation for a liquid−air interface can be expressed as

$$D(\omega) = L(\gamma)\, T(\tilde{\epsilon}) - C_B(\rho,\eta;\epsilon_2) \tag{7}$$

$$L(\gamma) = (\gamma + \tilde{B}q^2)q^2 + i\omega\eta(q + m) - \rho\omega^2/q \tag{9}$$

$$C_B(\rho,\eta;\tilde{\lambda}) = [\eta\omega(q - m) + i\tilde{\lambda}q^3]^2 \tag{10}$$

where $\tilde{B} = B + iB'$ accounts for the contribution of the bending mode and $\tilde{\lambda} = \lambda + i\lambda'$ accounts for the coupling between the bending and the longitudinal modes. The values of λ and B are linked to the elasticity and the thickness of the monolayer h_0 by simple relationships:

$$\lambda \sim \epsilon h_0; \quad B \sim \epsilon h_0^2 \tag{11}$$

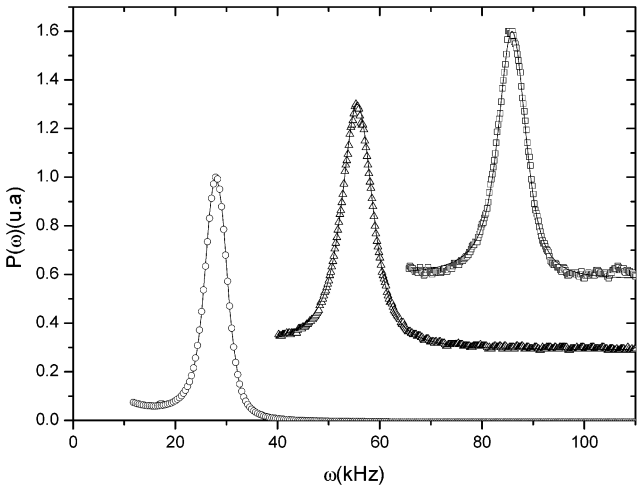

Figure 12. Best fits (continuous lines) of the SQELS spectra using the theory of Buzza et al. for the DB3 monolayer at $q = 217.3$ cm^{-1} and 25 °C and for three different surface pressures Π in mN m^{-1}: ○, 0.44; △, 5.53; □, 8.42. For the sake of clarity, the spectra have been shifted 30 kHz and 0.3 au. The theory fits the spectra with nonnegative values of the dilational viscosity for $\Pi \leq 8.5$ mN m^{-1}. However, negative apparent values of κ are still needed for higher surface pressures.

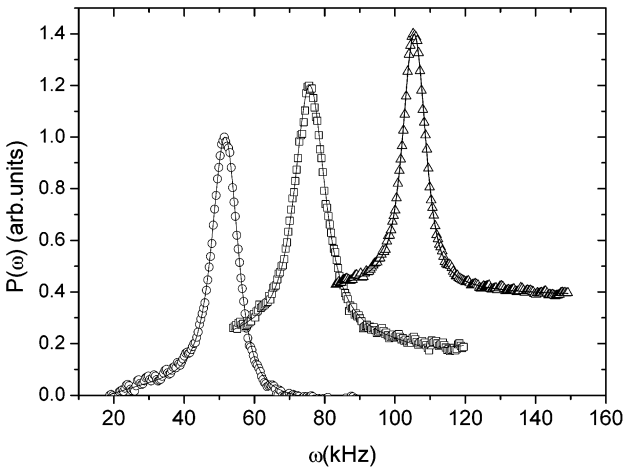

Figure 13. Best fits (continuous lines) of the SQELS spectra using the theory of Hennenberg with $\epsilon \approx \epsilon_0$. Monolayers of TB2 at 25 °C: ○, $q = 334.5$ cm^{-1}, and for three different surface pressures Π in mN m^{-1}: ○, 0.5; □, 4.8; △, 8.0. For the sake of clarity, the spectra have been shifted 20 kHz and 0.2 au.

λ' and B' are very small and have been considered as negligible. The expressions of $T(\tilde{\epsilon})$ and $P_z(q,\omega)$ are given by eqs 3 and 6, respectively.

The SQELS spectra of the DB3 copolymer for $\Pi = 15$ mN m^{-1} are fitted equally well with Buzza's equation (with $\kappa \approx 0$) than with eq 1 (with $\kappa < 0$) if a monolayer thickness of 10 μm is considered. The best fit leads to $\lambda = 0.123$ N and $B = 0.009$ mN m^{-1} and values of ϵ and κ which are indistinguishable from those obtained with eq 1. In the case of the monolayers of TB2 the theoretical spectrum derived from eqs 7−11 are able to fit very well the experimental spectra (see Figure 12). However a monolayer thickness of 40 μm is needed to obtain $\kappa \approx 0$ for $\Pi = 0.55$ and for $\Pi = 4.8$ mN m^{-1}. Even for such an unphysical value of the thickness, negative values of κ are obtained for $\Pi \geq 8.5$ mN m^{-1}. We have recently reported similar conclusions for monolayers of a PEO−PPO−PEO copolymer.[42]

Comparison with Hennenberg's Theory.[48] As discussed above, negative apparent dilational viscosities appear under conditions where the monolayers have a continuous layer of PS. This makes the interface nonattractive for the PEO segments, thus inducing the existence of a depletion layer. Since the width of the depletion layer is of the same order of magnitude as the penetration length of the capillary waves m,[3] these waves would travel through a region with a PEO concentration gradient. Hennenberg et al.[48] have shown that such situation introduces a new term in the Marangoni forces associated mainly with surface dilation. We have shown that this contribution leads to a new coupling term in the dispersion equation, which can be expressed as

$$D(\omega) = L(\gamma)\ T(\tilde{\epsilon}) - C_H(\rho,\eta;\epsilon_2) \qquad (12)$$

where the longitudinal (L) and the transversal (T) terms are the same as in eqs 2 and 3, and

$$C_H(\rho,\eta;\epsilon_2) = [i\omega\eta(q-\mu) + \epsilon_2 q^2]^2 \qquad (13)$$

Notice that if $\epsilon_2 = 0$, eq 12 reduces to eq 1. The effect of ϵ_2 is to increase the coupling between capillary and dilational modes. As a consequence, when fitting SQELS spectra, the effect of $\epsilon_2 > 0$ is qualitatively similar to that of negative effective values of the dilational viscosity. The values of κ and ϵ_2 are highly correlated; thus, it is possible to fit the experimental spectra using different sets (ϵ, κ, ϵ_2).

The SQELS spectra of the DB3 copolymer for $\Pi = 15$ mN m^{-1} are fitted equally well with Buzza's equation (with $\epsilon \approx \epsilon_0$) and with eq 1 (with $\kappa < 0$). Figure 13 shows the results of the fittings to some of the SQELS spectra of TB2 monolayers. As can be observed, the theory is able to fit the experimental results within the experimental precision. The values obtained for ϵ_2 are of the same order of magnitude as the corresponding values of ϵ. Contrary to Buzza's theory, where the thickness of the monolayer has a clear microscopic meaning, so far it is not possible to discuss the values of ϵ_2 in terms of any molecular parameters. It is, however, important to point out that Hennenberg's theory is able to fit the SQELS spectra of the DB3 and TB2 monolayers at high grafting densities with positive values of κ, while negative apparent dilational viscosities were still necessary when Buzza's theory is used, even for unrealistically large values of the thickness of the monolayer.

Conclusions

The surface pressure of monolayers of three diblock PS-*b*-PEO copolymers has been measured in the 5−35 °C temperature interval. The number of EO units N_{PEO} ranges from 952 to 1066, while the number of PS units was $59 \leq N_{PS} \leq 158$. The Π vs area curves are coincident when the area axis is normalized with N_{PEO}. The shape of this generalized isotherm is in agreement with the predictions of the scaling and the self-consistent-field theories, and the transition from the self-similar structure SSL to the quasi-brush was found to be continuous. N_{PS} was found to have no influence on determining the surface pressure at which the transition takes place Π_{Pl}. However, the increase of N_{PS} reduces the slope of the transition region of the isotherm. For the copolymer with the largest value of N_{PS}, the monolayer collapses at Π_{Pl}. In the case of PEO-*b*-PS-*b*-PEO triblock copoly-

mers, the surface pressure vs area curves did not collapse into the same curve when the area axis was normalized by N_{PEO}. Again, the isotherm for the copolymer with the largest value of N_{PS} collapses at Π_{Pl}. Temperature was not found to have a significant influence on any of the copolymers. In the semidilute regime, the Π vs A curves can be described by a scaling law with an exponent which is intermediate between that of 2D and 3D chains in good-solvent conditions. However, for the TB3 triblock monolayer such an exponent corresponds to poor-solvent conditions. This and the fact that the monolayer collapses at Π_{Pl} probably indicates that the behavior is dominated by the PS blocks.

The dynamic elasticity ϵ and the dilational viscosity κ have been obtained by combining oscillatory barrier, electrocapillary wave, and light scattering experiments through the 0.01 Hz $\leq \omega \leq$ 100 kHz frequency interval. In all the cases ϵ is larger than the equilibrium compressibility modulus ϵ_0, pointing out the viscoelastic character of the monolayers. Both ϵ and ϵ_0 show a maximum for grafting densities Γ close to those at which the SSL begins to be formed for each monolayer. They then decrease as Γ increases because the number of tails and loops of the PEO chains that protrude into the water subphase increases. These tails and loops are very effective in dissipating the stress of the monolayer. ϵ and ϵ_0 reach a minimum near the SSL−quasi-brush transition, and then they increase again for those monolayers that do not collapse at Π_{Pl}.

The frequency dependence of ϵ and $\omega\kappa$ at the grafting density Γ^{**} point out that there is only one relaxation process centered in the 0.1−1 kHz region, whose shape can be described by a Maxwell function. However, the amplitude of the Maxwell mode for ϵ is much larger than for $\omega\kappa$. This behavior is rather different from the one found for a PEO-*b*-PPO-*b*-PEO copolymer, which shows a Lucassen−van den Tempel relaxation at much lower frequencies (ca. 1 mHz), in addition to a Maxwell-like relaxation in the 0.1−1 kHz range.

The capillary wave experiments lead to negative apparent values of κ for the TB3 monolayers. The analysis of the SQELS spectra in terms of the theory of Buzza allows us to fit the experimental results with $\kappa \approx 0$ for $\Pi \leq 8$ mN m^{-1} using unphysical values for the thickness of the monolayer. However, this theory still leads to $\kappa < 0$ for higher pressures. What is more, Hennenberg's theory is able to fit the SQELS spectra of the DB2 and TB3 monolayers with positive values of the dilational viscosity. Finally, it is not possible to discuss the values of the coupling parameter ϵ_2 in terms of any molecular variable.

Acknowledgment. This work was supported in part by MCyT under Grant BQU2000-0786 and by a Del Amo project. S. Rivillon gratefully acknowledges a Marie Curie postdoctoral fellowship from E.U. We are grateful to Prof. D. Langevin for allowing us to use the ellipsometer.

References and Notes

(1) Alexander, S. *J. Phys. (Paris)* **1977**, *38*, 977.
(2) Halperin, A. *Europhys. Lett.* **1987**, *4*, 439.
(3) Fleer, G. J.; Cohen Stuart, M. A.; Scheutjens, J. M. H. M.; Cosgrove, T.; Vincent, B. *Polymers at Interfaces*: Chapman-Hall: Cambridge, 1993.
(4) Daoud, M. *Colloids Surf. A* **1994**, *86*, 41.
(5) Richards, R. W.; Rochford, B. R.; Webster, J. R. P. *Polymer* **1997**, *38*, 1169.
(6) Prokop, R. M.; Hair, M. L.; Neumann, A. W. *Macromolecules* **1996**, *29*, 5902.
(7) Rother, G.; Findenegg, G. H. *Colloid Polym. Sci.* **1998**, *276*, 496.
(8) Xu, Z.; Holland, N. B.; Marchant, R. E. *Langmuir* **2001**, *17*, 377.
(9) Malzert, A.; Boury, F.; Saulnier, P.; Benoît, J. P.; Proust, J. E. *Langmuir* **2001**, *17*, 2001.
(10) Bowers, J.; Zarbakhsh, A.; Webster, J. R. P.; Hutchings, L. R.; Richards, R. W. *Langmuir* **2001**, *17*, 131.
(11) Currie, E. P. K.; Leermakers, F. A. M.; Cohen Stuart, M. A.; Fleer, G. J. *Macromolecules* **1999**, *32*, 487.
(12) Szleifer, I. *Europhys. Lett.* **1998**, *44*, 721.
(13) Ligoure, C. *J. Phys. II* **1993**, *3*, 1607.
(14) de Gennes, P. G. *Macromolecules* **1980**, *13*, 1069.
(15) Kent, M. S.; Lee, L. T.; Farnoux, B.; Rondelez, F. *Macromolecules* **1992**, *25*, 6240.
(16) Kent, M. S.; Lee, L. T.; Factor, B. J.; Rondelez, F.; Smith, G. S. *J. Chem. Phys.* **1995**, *103*, 2320.
(17) Kent, M. S.; Majewski, J.; Smith, G. S.; Lee, L. T.; Satija, S. *J. Chem. Phys.* **1998**, *108*, 5635.
(18) Aubouy, M.; Guiselin, O.; Raphaël, E. *Macromolecules* **1996**, *29*, 7261.
(19) Bijsterbosch, H. D.; de Haan, V. O.; de Graaf, A. W.; Mellema, M.; Leermakers, F. A. M.; Cohen Stuart, M. A.; van Well, A. A. *Langmuir* **1995**, *11*, 4467.
(20) Gonçalves da Silva, A. M.; Filipe, E. J. M.; d'Oliveira, J. M. R.; Martinho, J. M. G. *Langmuir* **1996**, *12*, 6547.
(21) Fauré, M. C.; Bassereau, P.; Carignano, M. A.; Szleifer, I.; Gallot, Y.; Andelman, D. *Eur. Phys. J. B* **1998**, *3*, 265.
(22) Fauré, M. C.; Bassereau, P.; Lee, L. T.; Menelle, A.; Lhevender, C. *Macromolecules* **1999**, *32*, 8538.
(23) Gonçalves da Silva, A. M.; Simoes Gamboa, A. L.; Martinho, J. M. G. *Langmuir* **1998**, *14*, 5327.
(24) Dewhurst, P. F.; Lovell, M. R.; Jones, J. L.; Richards, R. W.; Webster, J. R. P. *Macromolecules* **1998**, *31*, 7851.
(25) Cox, J. K.; Yu, K.; Eisenberg, A.; Lennox, R. G. *Phys. Chem. Chem. Phys.* **1999**, *1*, 4417.
(26) Richards, R. W.; Rochford, B. R.; Taylor, M. R. *Macromolecules* **1996**, *29*, 1980.
(27) Huang, Q. R.; Wang, C. H. *Langmuir* **1996**, *12*, 2679.
(28) Peace, S. K.; Richards, R. W.; Williams, N. *Langmuir* **1998**, *14*, 667.
(29) Alexander, M.; Richards, R. W. *J. Phys. Chem. B* **2000**, *104*, 9179.
(30) Esker, A. R.; Zhang, L. H.; Sauer, B. B.; Lee, W.; Yu, H. *Colloids Surf.* **2000**, *171*, 131.
(31) Noskov, B. A.; Akentiev, A. V.; Miller, R. *J. Colloid Interface Sci.* **2002**, *247*, 117.
(32) Cao, B. H.; Kim, M. W. *Europhys. Lett.* **1995**, *29*, 555.
(33) Milling, A. J.; Hutchings, L. R.; Richards, R. W. *Langmuir* **2001**, *17*, 5297.
(34) Monroy, F.; Ortega, F.; Rubio, R. G. *Phys. Rev. E* **1998**, *58*, 7629.
(35) Monroy, F.; Rivillon, S.; Ortega, F.; Rubio, R. G. *J. Chem. Phys.* **2001**, *115*, 530.
(36) Langevin, D. *Light Scattering by Liquid Surfaces and Complementary Techniques*; Dekker: New York, 1992.
(37) Dorgan, J. R.; Stamm, M.; Toprakcioglu, C.; Jérôme, R.; Fetters, L. J. *Macromolecules* **1993**, *26*, 5321.
(38) Kuzmenka, D. J.; Granick, S. *Macromolecules* **1988**, *21*, 779.
(39) Tompkins, H. G. *A User's Guide to Ellipsometry*; Academic Press: San Diego, 1993.
(40) Muñoz, M. G.; Monroy, F.; Ortega, F.; Rubio, R. G.; Langevin, D. *Langmuir* **2000**, *16*, 1094.
(41) Monroy, F.; Ortega, F.; Rubio, R. G. *J. Phys. Chem. B* **1999**, *103*, 2061.
(42) Muñoz, M. G.; Monroy, F.; Hernández, M.-P.; Ortega, F.; Rubio, R. G.; Langevin, D. *Langmuir* **2003**, *19*, 2147.
(43) Noskov, B. A. *Colloid Polym. Sci.* **1995**, *273*, 263.
(44) Noskov. B. A.; Akentiev, A. V.; Loglio, G.; Miller, R. *J. Phys. Chem. B.* **1999**, *104*, 7923.
(45) Lucassen-Reynders, E. H.; Lucassen, J. *Adv. Colloid Interface Sci.* **1969**, *2*, 347.
(46) Buzza, D. M. A.; Jones, J. L.; McLeish, T. C. B.; Richards, R. W. *J. Chem. Phys.* **1998**, *109*, 5008.
(47) Muñoz, M. G.; Luna, L.; Monroy, F.; Rubio, R. G.; Ortega, F. *Langmuir* **2000**, *16*, 6657.

MA021260Z